Effective dose and Effective risk from post-SPECT imaging of the lumbar spine

Abstract

Purpose

Planar bone scans play an important role in the staging and monitoring of malignancy and metastases. Metastases in the lumbar spine are associated with significant morbidity, therefore accurate diagnosis is essential. Supplementary imaging after planar bone scans is often, required to characterise lesions, however, this is associated with additional radiation dose. This paper provides information on the comparative effective dose and effective risk from supplementary lumbar spine radiographs, low-dose CT (LDCT) and diagnostic CT (DCT).

Method

Organ dose was measured in a phantom using thermo-luminescent dosimeters. Effective dose and effective risk were calculated for radiographs, LDCT, and DCT imaging of the lumbar spine.

Results

Radiation dose was 0.56mSv for the antero-posterior and lateral lumbar spine radiographs, 0.80mSv for LDCT, and 3.78mSv for DCT. Additional imaging resulted in an increase in effective dose of 12.28%, 17.54% and 82.89%for radiographs, LDCT and DCT respectively. Risk of cancer induction decreased as age increased. The difference in risk between the modalities also decreased. Males had a statistically significant higher risk than female patients ($p=0.023$) attributed to the sensitive organs being closer to the exposed area.

Conclusion

Effective Dose for LDCT is comparable to radiographs of the lumbar spine. Due to the known benefits image fusion brings it is recommended that LDCT replace radiographs imaging for characterisation of lumbar spine lesions identified on planar bone scan. DCT is associated with significantly higher effective dose than LDCT. Effective risk is also higher and the difference is more marked in younger female patients.

Introduction

Planar whole-body bone scintigraphy (BS) using Technetium 99m phosphates or phosphonates [1] and a gamma camera continues to play an important role in the staging and monitoring of malignant disease due to its ability to demonstrate lesions earlier than conventional radiographic methods [1, 2]. The lumbar spine is a common site for bony metastases arising from primary tumour sites in the prostate and breast due to venous drainage into the vertebral plexus [3]. Metastases in the spine are associated with significant morbidity, therefore accurate and early diagnosis is important for effective patient management [3-5]. Multiple lesions in the spine detected using BS does not provide a definitive diagnosis but are suggestive of metastatic disease [6]. When solitary spinal lesions are discovered a definitive diagnosis is challenging due to the spectrum of potential pathological processes. These cases are often referred for additional imaging to localise and/or characterise them.

Over a decade ago research lead to a significant change in scanning technique [1]. BS evolved to include single photon emission computed tomography (SPECT) and later computed tomography (CT), with SPECT-CT now regarded as an essential tool in diagnosing and assessing metastatic bone disease [7]. Prior to tomographic imaging, patients were referred for supplementary imaging to help localise or characterise a lesion: typically using conventional plain radiography, CT or MRI. Hybrid imaging systems now allow fusion of CT and SPECT images, providing the clinician with physiological data overlaid on anatomical information. This removes the necessity for side-by-side comparison.

The benefits of image fusion in nuclear medicine imaging are covered extensively in literature, which reports an increase in the accuracy, sensitivity, specificity and diagnostic confidence [8-11]. These benefits are associated with additional risk, since supplementary imaging requires additional radiation dose to the patient. Research has shown that the additional dose from CT acquisitions acquired as part of a SPECT-CT study are not insignificant and on occasions can exceed the dose from the administration of the radiopharmaceutical. Increases in effective dose of between 2% and 600% are reported [12].

The early use of CT in combination with SPECT was aimed at attenuation correction (AC) and consisted of a CT component with fixed acquisition parameters. These scanner types are frequently referred to as low-dose with an effective dose 80-85% lower than diagnostic quality CT scans [12-15]. Diagnostic CT (DCT) can be used to aid diagnosis rather than correcting the emission data alone [16] and also provide localisation data [17]. Regardless of the modality the additional dose has to be taken into account in the justification of the exposure [18, 19]. Justification should ensure that the benefit of the exposure outweighs the potential risk from the additional exposure.

The additional dose from the CT component of SPECT-CT has been investigated [12-15]. Larkin et al [14], Sharma et al [12] and Montes et al [15] use the dose length product and conversion (*k*) factors to calculate effective dose. Hara et al [13] measured organ dose with thermoluminescent dosimeters (TLD) however only organs within the primary beam were measured. The paper does not recreate the clinical situation where organs outside the primary beam would be subject to scatter radiation.

The aims of our research are to calculate effective dose and effective risk from imaging of the lumbar spine using radiographs, LDCT and DCT. From this data the additional dose over BS alone are

calculated. Male and female effective risk will be compared to figures from SPECT alone and SPECT plus supplementary imaging.

Method

Using an adult dosimetry phantom (ATOM 701D (CIRS Inc, Virginia USA)), organ dose was measured using thermo-luminescent dosimeters (TLD100H (Thermo Fisher Scientific Massachusetts, USA)) . Effective dose and effective risk were calculated as described below. Three imaging systems were used in this study. The first was radiographs using a Wolverson Acroma General X-ray system (Willenhall, UK) with an Agfa computed radiography system (Agfa Health Care, Mortsel, Belgium). The second was multi-detector diagnostic CT (DCT) (Toshiba Aquillion 16, Toshiba Medical Systems Corporation, Tochigi-ken, Japan). The third was a low-specification CT component from a hybrid SPECT-CT system (low-dose CT (LDCT)) (GE Infinia Hawkeye 4, GE Healthcare, Little Chalfont, UK). Imaging equipment quality control for tube output and automatic exposure devices met the required standards and manufacturer guidelines [20-22]. Air-calibrations for the two CT systems were performed as part of the warm-up procedures. The imaging parameters were based on those used in the clinical environment and had undergone an optimisation process through audits of image quality and diagnostic reference levels. The automatic exposure control for radiographs and the mA modulation function for the DCT were used. For LDCT exposure factors for an average sized patient were used (Table 2).

The Phantom

The anthropomorphic dosimetry phantom consists of 39 contiguous sections of differing density epoxy resin (representing bone, lung and soft tissue) that when put together make up the head and torso of an adult male. TLD locations were positioned for precise dosimetry of specific internal organs. Whole body effective dose calculation was completed using the ATOM 701-D configuration that utilises a total of 271 TLDs over 22 organs [23, 24].

For AP and lateral lumbar spine, the area of interest adhered to criteria set out in a standard radiography technique book [25]. The medial-sagittal and medial-coronal planes, the field of view and the centre for antero-posterior and left lateral projections of the lumbar spine were marked onto the phantom's surface with permanent marker pen and radiolucent markers were used to aid positioning of the CT acquisitions (Figure 1).

Figure 1 marking the phantom for AP and left lateral lumbar spine projections and CT lumbar spine.

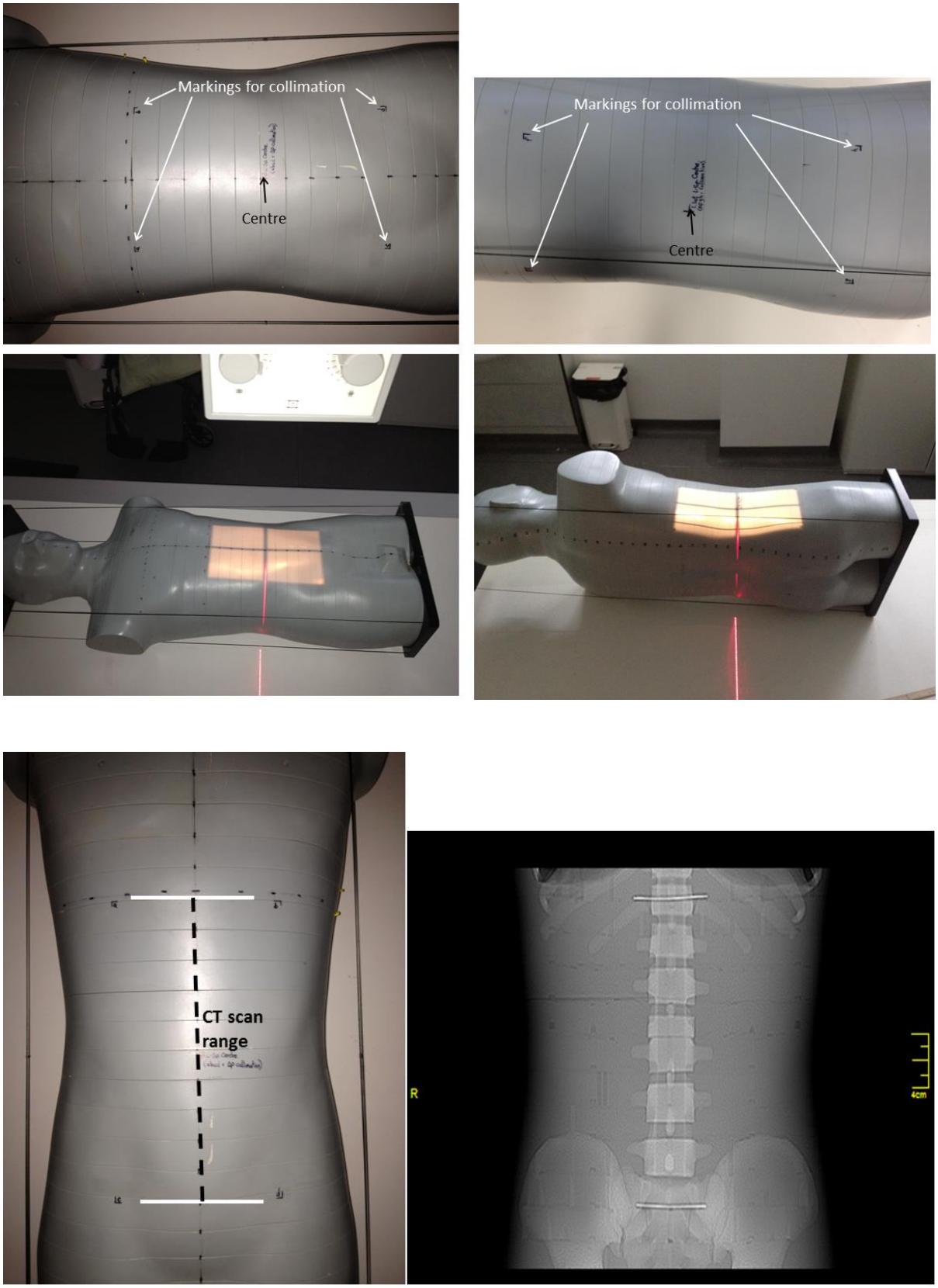

Positioning the phantom for the LDCT acquisition on the SPECT-CT hybrid system involved the use of external positioning aids. Commercially available laser spirit levels allowed the phantom to be centrally positioned on the table and parallel to its long axis. A scout view is not routinely acquired as planning of the CT range is performed on patients using the emission data. To ensure close replication of clinical practice the scan range was determined by setting a zero refresh rate on the positioning monitor and placing a ^{57}Co source on the markings on the phantom until it was visible on the scanner's positioning monitor. These two points corresponded to the upper and lower limit of the CT acquisition. To ensure the use of the unsealed source in this manner did not contribute to the dose recorded by the TLDs, the dose recorded in 5 seconds at a distance of 1 cm in air was calculated. Using the reference activity of 3.7 MBq for the Cobalt source resulted in 6.53 x 10^{-4} mGy. This value is below the sensitivity of the TLDs and so was considered negligible when calculating the dose from the TLDs in the phantom.

Thermoluminescent dosimeters

The TLDs were read using a Harshaw 3500 manual TLD reader one day after their exposure. To ensure accuracy and reproducibility the TLDs were subjected to quality control checks. The TLDs were annealed by heating to 240^{o}C for 10 minutes. They were then exposed to a uniform field of X-radiation using a general x-ray unit, processed and grouped together into batches of similar response. To ensure repeatability the batches were annealed and exposed to the same uniform field and their responses compared. A paired student t-test was performed and there was no significant difference in the responses of the two exposures ($p>0.1$). The inter batch coefficient of variance was calculated and was less than 2.0%. Calibration was performed on each batch using a general x-ray unit at energies of 120kV and 80kV to correspond with settings used in the imaging protocols [26]

The TLDs were positioned in the phantom at locations of the organs identified in ICRP 103 (Table 1) at the organ positions specified by the manufacturer [23, 24, 27]. Five TLDs remained with the phantom at all times apart from during image acquisition for background correction.

Table 1 Number of TLDs used in critical organs

Organ	Number of TLD	Organ	Number of TLD
Adrenals	2	Liver	30
Bladder	16	Lungs	36
Brain	11	Oesophagus	3
Breast	2	Pancreas	5
Active bone Marrow	85 Clavicle 20, Cranium 4 Cervical Spine† 2 Femora 4 Mandible◊× 6 Pelvis 18	Prostate	3

	Ribs 18 Sternum 4 Thoraco-lumbar Spine 9		
Eyes*	2	Spleen	14
Gall Bladder	5	Stomach	11
Heart	2	Testes	2
Intestine (Small and large)	16 Colon 11 Small intestine 5	Thyroid	10
Kidneys	16	Thymus	4

* Not included in effective dose calculations

† TLDs located in the anterior of C2 and upper oesophagus were used to calculate extra thoracic organ dose

◊ TLDs located in the left and right lingula of the mandible and to the left and right of the sublingual fossa were used to calculate salivary gland organ dose

× TLDs located in the left and right lingula of the mandible were used to calculate oral mucosa organ dose

To increase the signal to noise ratio of the TLD readings three complete exposures were performed using the acquisition parameters shown in Table 2. This resulted in a cumulative dose being recorded on the TLDs which was divided by three to give a dose per exposure. Effective dose for the three modalities was calculated using tissue weighting factors listed in ICRP report 103 [27] (see Table 3). Statistical analysis was performed using two-way ANOVA with post hoc testing with Bonferroni correction.

Table 2 Parameters used for imaging the lumbar spine in CR, diagnostic CT and Low Dose CT

Radiographs			
	kV	AED chamber	Post mAs
AP	75	Central	Mean 60 (SD=0)
Left lateral	80	Central	Mean 72 (SD=0)

Diagnostic CT			
Scan Projection Radiograph			
	kV	mAs	Scan range
AP	120	150	250 mm
Left Lateral	120	45	250 mm

Axial scan						
Mode	kV	mA	Rotation (s)	Pitch	Detector range	Scan range
Helical	120	Auto Lower: 100 Upper: 450 SD: 7.5	0.75	0.938	16 mm 16x1 mm	245 mm Upper- Mid T12 Lower- Upper S3

Low Dose CT						
Mode	kV	mA	Rotation (rotations per minute)	Pitch (distance per rotation) (mm)	Detector range	Scan range
Helical	120	2.5	2	1.9	20 mm 4 x 5 mm	245 mm Upper- Mid T12 Lower- Upper S3

Table 3 Tissue weighting factors from ICRP report 103 [18]

Tissue	W_T	$\sum w_T$
Bone Marrow, Colon, Lung, Stomach, Breast, Remainder tissues*	0.12	0.72
Gonads	0.08	0.08
Bladder, Oesophagus, Liver, Thyroid	0.04	0.16
Bone Surface[×], Brain, Salivary glands, Skin[×]	0.01	0.04
*adrenals, extrathoracic region, gallbladder, heart, kidneys, lymphatic nodes[×],oral mucosa, pancreas, prostate, small intestine, spleen, thymus		
[×]excluded in this study.		

Risk calculations were carried out following a method described by Brenner [28, 29]. Lifetime risk of cancer incidence figures were obtained from Wall et al [30]. The sum of the product of the measured organ dose (mGy) and the life time risk of cancer incidence for that organ (percentage per mGy) gave the effective risk. Resources dictated that the phantom used within this study was male, however by using TLD readings from locations that correspond with the gonads and uterus and excluding the male testes and prostate it was possible to calculate an effective risk for females.

Organ and effective dose from the administration of 800 MBq ^{99m}Tc labelled phosphate or phosphonates was calculated using dose per unit activity (mSv/MBq) from Bombardieri et al [1]. Comparisons were made between the dose from additional imaging and the initial bone scan acquisition.

Results

A comparison of dose data as displayed by the modalities is shown in Table 4. DLP and CTDi are significantly higher for DCT compared to LDCT. This supports the findings of the dosimetry data that DCT will result in a higher dose. Comparison of the effective dose from the three supplementary imaging techniques is shown in Figure 2. Imaging using DCT results in a higher effective dose compared to radiographs and LDCT. The error bar for DCT is larger due to the 2% error in the TLDs being applied to a larger dose reading.

Table 4 Comparison of DAP/DLP and CTDi

	Radiographs	LDCT	DCT
DAP (mGy.cm^2)	*2873*	--	--
DLP (mGy.cm)	--	96.0	349.6
CTDi (mGy)	--	3.97	20.0

Figure 2 Effective dose from the supplementary imaging modalities

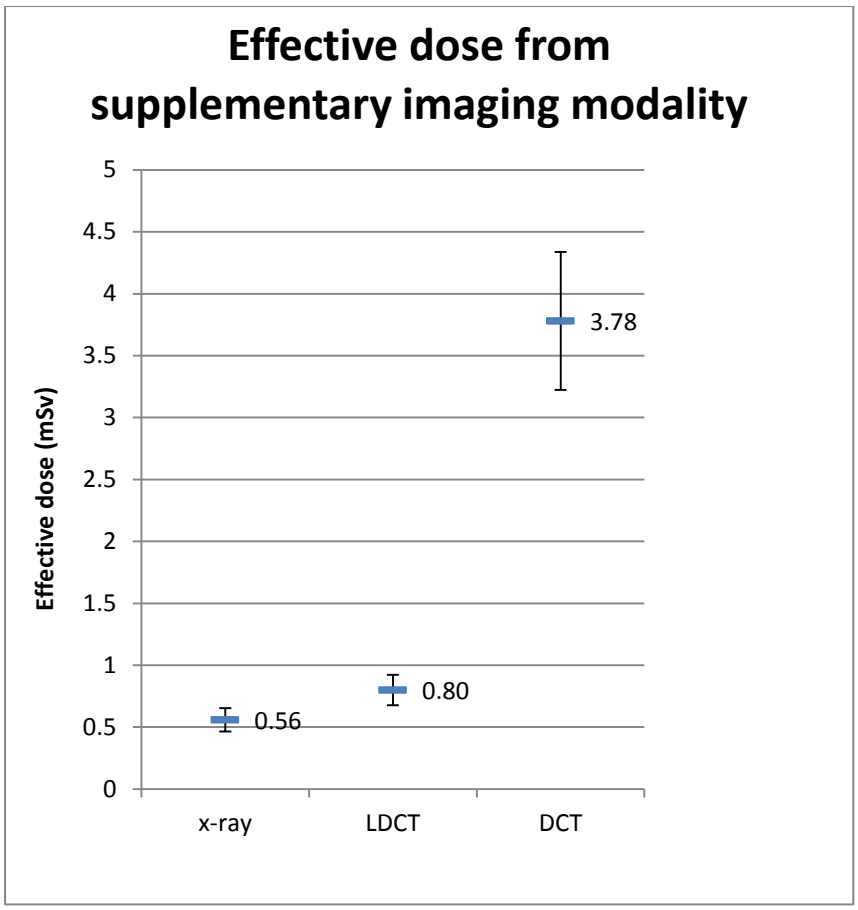

Effective dose is calculated from the sum of the weighted organ doses and does not indicate the difference to individual organs. Table 5 and

Table 6 illustrate the organ dose from and increase due to the supplementary imaging modality compared to the calculated organ dose from the administration of the radiopharmaceutical. Certain organs, for example the colon, liver and stomach, exhibit a large increase due to the low uptake of radiopharmaceutical but are situated within the scan range. There is a consistent difference in organ dose between DCT and LDCT and DCT and radiographs showing the distribution of the organ dose is consistent for the supplementary imaging modality.

Table 5 comparison of organ dose from the three supplementary modalities compared to the Bone scan (800MBq phosphate or phosphonate).

	Absorbed dose (mGy)			
Organ	**BS**	**Radiographs**	**LDCT**	**DCT**
Active bone marrow	7.36	0.15	0.33	1.75
Bladder	38.40	0.55	0.59	3.83
Brain	1.36	0.00	0.00	0.01
Breast	0.57	0.04	0.07	0.44
Colon	2.16	1.58	2.12	9.00
Liver	0.96	1.42	1.42	7.23
Lungs	1.04	0.11	0.15	1.16
Oesophagus	0.80	0.06	0.11	0.72
Stomach	0.96	1.29	2.14	9.86
Thyroid	1.04	0.01	0.02	0.09
Remainder organ	1.52	0.79	1.10	5.21

.

Table 6 Increase in organ dose for the organs

	Absorbed dose (mGy)						
		BS & Radiographs		BS & LDCT		BS & DCT	
Organ	**BS only**	**mGy**	**% increase**	**mGy**	**% increase**	**mGy**	**% increase**
Active bone marrow	7.36	7.51	2.09	7.69	4.49	9.11	23.76
Bladder	38.40	38.95	1.43	38.99	1.55	42.23	9.97
Brain	1.36	1.36	0.04	1.36	0.02	1.37	0.73
Breast	0.57	0.61	7.72	0.64	12.39	1.01	77.86
Colon	2.16	3.74	73.26	4.28	98.2	11.16	16.54
Liver	0.96	2.38	147.58	2.38	147.73	8.19	753.27
Lungs	1.04	1.15	10.14	1.19	14.83	2.20	111.76
Oesophagus	0.80	0.86	7.87	0.91	13.93	1.52	89.4
Stomach	0.96	2.25	134.74	3.10	222.95	10.82	1027.35
Thyroid	1.04	1.05	0.83	1.06	2.23	1.13	8.81
Remainder	1.52	2.31	52.04	2.62	72.41	6.73	342.47

Using data published by Wall et al[30], life time cancer risk for all cancers and cancers of the organs identified in

Table 6 were calculated. Comparison of risk between bone scan (BS) only, BS with conventional radiography, BS with low dose CT, and BS with diagnostic CT from 40 to 89 years are shown in Figure 3,

Figure 4 and Figure 5.

Figure 3 Effective risk from exposure for all cancers for a Euro-American population

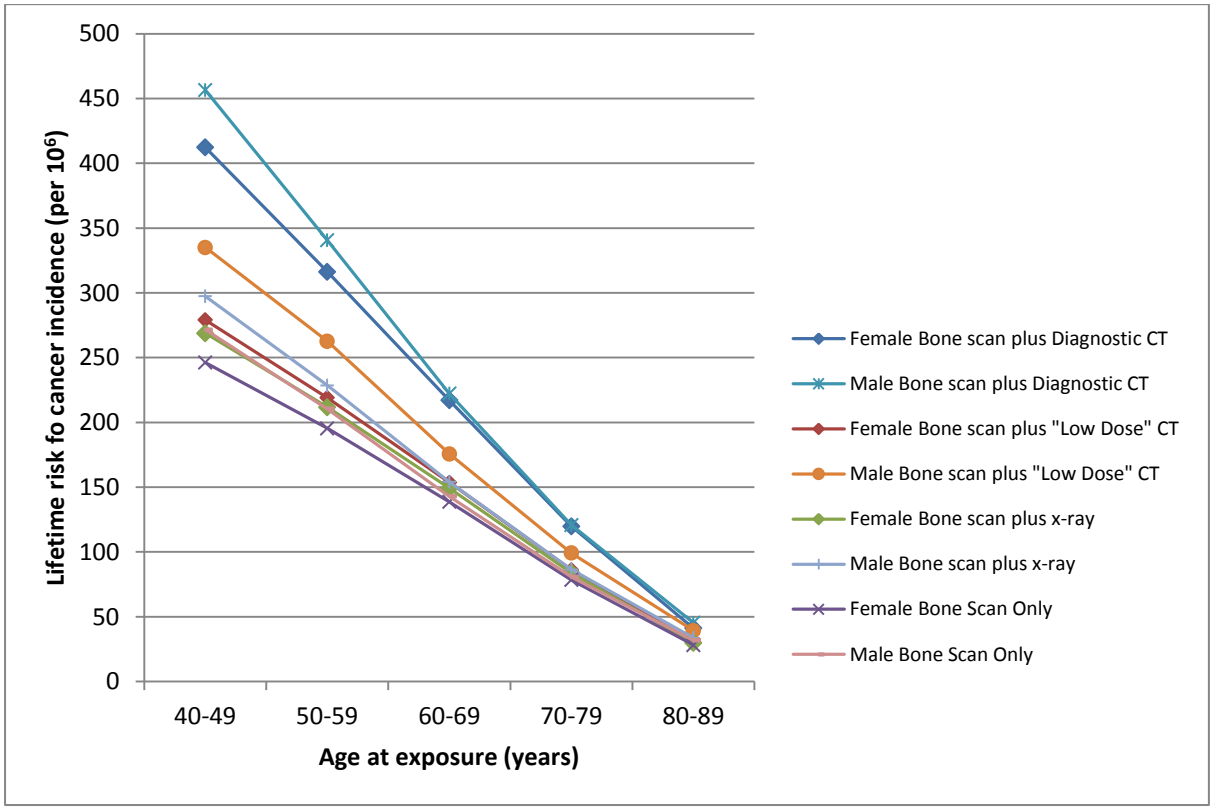

Figure 4 Effective risk from exposure for all cancers for a female Euro-American population

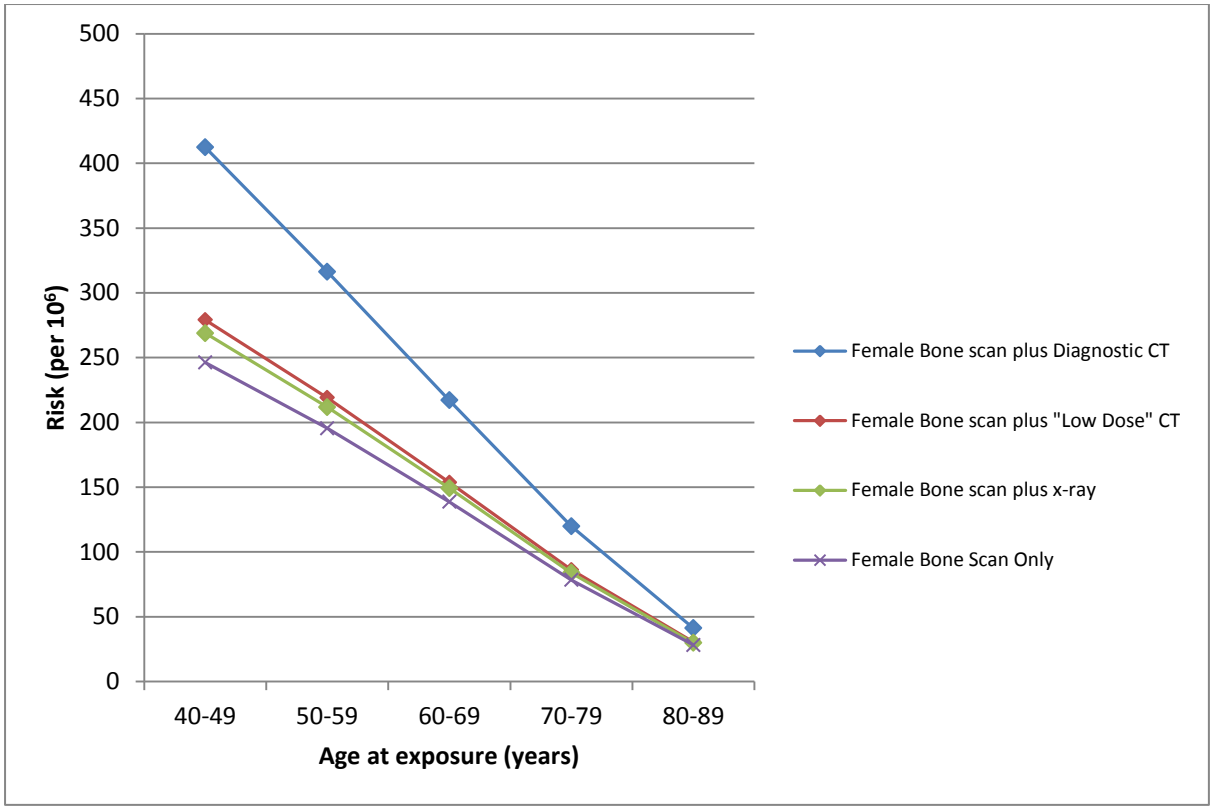

Figure 5 Effective risk from exposure for all cancers for a male Euro-American population

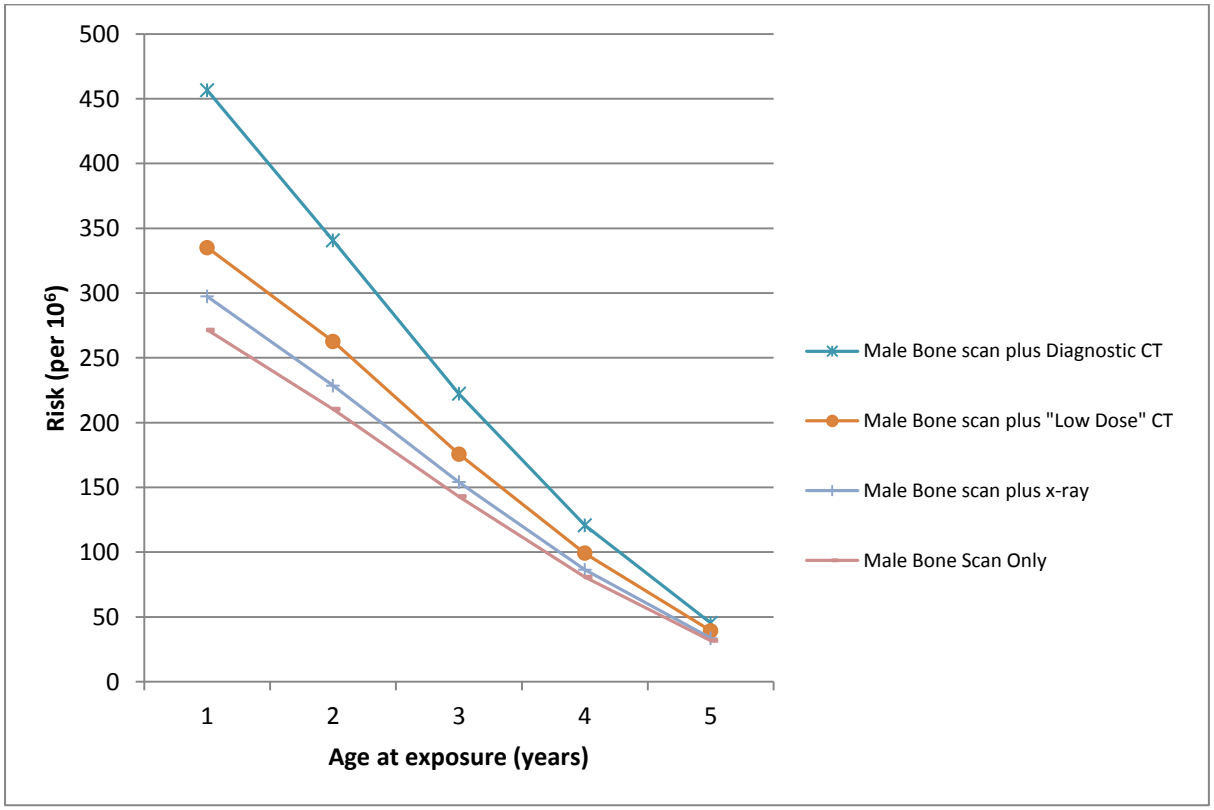

Discussion

Image fusion has been shown to increase accuracy and reporter confidence [8-11]. It has been suggested that DCT that can further aid diagnostic decisions due to its ability to acquire and display submillimetre structures thus showing the accurate location and internal architecture of a lesion [31-35]. To date little data directly comparing the additional organ and effective dose and effective risk for all available supplementary imaging options has been published. Our results show that the effective dose from lumbar spine imaging using radiographs was 0.56 mSv (±0.09), LDCT 0.80 mSv (±0.12) and DCT was 3.78 mSv (±0.56), The calculated effective dose from the administration of 800 MBq of ^{99m}Tc labelled phosphate or phosphonate is 4.56 mSv. Thus the additional effective dose from supplementary imaging is 12.3% for radiographs, 17.5% for LDCT and 82.9% for DCT.

This increase in effective dose was hypothesised and this result is in agreement with other research [12-14, 36]. However consideration of effective dose does not provide the narrative as it is not apparent which organs contribute to this increase.

Table 6 shows there are increases in organ dose from the supplementary imaging techniques. Comparison of organ doses using two way ANOVA showed that there was a statistically significant difference between the three options (p=0.001). Post hoc testing with Bonferroni correction showed that there was a statistically significant difference between BS & DCT and BS & LDCT (p=0.001) and BS & DCT and BS & radiographs (p=0.001). There was no statistical difference between BS & LDCT and BS & radiographs (p=0.810). On this basis there is a strong rationale for the use of LDCT over radiographs for imaging the lumbar spine. There is no statistically significant increase in organ dose and literature suggests that accuracy and clinician confidence is increased when using LDCT compared with radiographs.

There is no change to the urinary bladder dose and there is a relatively small increase in dose (from 38.4 mGy to 42.23 mGy (9.91%) for BS & DCT, 38.99 (1.55%) for LDCT and 38.95 mGy (1.43%) for BS & radiographs). The stomach receives one of the lowest doses from the radiopharmaceutical (0.96 mGy). Following supplementary imaging this figure increases to 10.82 mGy (+1027.35%) for BS+DCT, 3.10 mGy (+222.95%) for BS & LDCT and 2.25 mGy (+134.74%) for BS & radiographs. These results are due to the organ being directly in the field of view when imaging the lumbar spine. While these results are specific to lumbar spine imaging they have shown that the supplementary imaging can significantly increase organ dose.

Effective dose is commonly used in medical imaging to compare the risks from different modalities or techniques. Effective dose should not be used to calculate risk to an individual patient or patient types as it does not consider the age of the patient. Effective risk is a method described by Brenner [28, 29, 37] and Wall [30] in which tissue weighting factors are replaced with organ-specific radiation-induced cancer risk , such as those published by The Nuclear and Radiation Studies board [38], and Wall [30]. Discussion about the use of effective dose and effective risk are beyond the remit of this article but are reported widely in literature [28-30, 37, 39-42].

Figure 4 and Figure 5 illustrate the difference in the lifetime risk of radiation induced cancer between the supplementary modalities with increasing age. The difference between these values does decrease with age and when comparison is made between the effective risk for patients over 70 the difference is very small. The higher organ doses for BS & DCT is reflected in the higher risks for these ages with an incidence of 217 per million exposures for females and 154 per million examinations for males.

A limitation of this study is that the whole of the lumbar spine was imaged by the three modalities. In clinical practice a localised CT scan based on the planar and SPECT bone scan could be performed as opposed to the whole lumbar spine. This would limit the exposure to the area of interest meaning that organ doses would be less. This is likely not to be the case for radiographs where the full lumbar spine would be imaged. In other words, LDCT would likely be lower than radiographs.

This study uses the standard adult male phantom for dosimetry measurements. External validity of the research could be improved with the use of a female anthropomorphic phantom. However initial comparison of risk between male and female shows that the figures for male patients are higher. The reason for the difference is due differences in the sensitivities of the tissues. Sensitive organs in the female patient such as the breast tissue receive very little additional dose in imaging the lumbar spine as these are outside the field of view. Also, the specific focus of this work is the lumbar spine; a lesion requiring further clarification in the thoracic spine would result in breast tissue receiving a higher dose and would affect effect risk. Further research into supplementary imaging of other common sites of bony pathology is therefore warranted.

In older patients there is little additional risk however, in younger patients, risk is greater. In patients over 70 the difference in risk from the additional imaging decreases to the point where performing a DCT instead of LDCT could be justified. DCT can provide diagnostic image quality and afford good diagnostic value in the characterisation of a lesion.

Even-Sapir et al [31] suggest that referral for and justification of DCT over LDCT should be taken on a case-by-case basis and the benefits of the higher image quality and therefore high dose balanced against the risks [31]. There are likely to be instances when higher resolution images are required and in these cases the higher dose and associated risk from DCT is justified. The diagnostic value of the supplementary imaging options is beyond this work but research has shown the benefit of supplementing SPECT with CT [8, 31, 43, 44]. Further research in the usefulness of higher dose/higher quality CT acquisitions compared to low dose would facilitate the risk/benefit discussion.

Accepted practice is to use CT as a supplementary imaging modality over radiographs due to the benefits image fusion brings [45-47]. Recent papers consider the use of 16 slice or higher CT scanners and they note that the improved image quality allows reporters to comment upon the internal structure of a lesion as well as identifying its location [8, 9, 31, 43, 44, 48]. The current work has shown acquisitions using DCT result in a statistically significant higher dose.

Conclusion

Our work demonstrates that a DCT acquisition result in an effective dose and effective risk that is significantly higher than a LDCT acquisition. The LDCT system used in our work has demonstrated a small increase in dose and risk compared with radiographs. However LDCT brings the benefits of improved diagnostic confidence and thus are recommended as the preferred choice of bone scan supplemental imaging for bony metastases.

References

1. Bombardieri E, Aktolun C, Baum RP, Bishof-Delaloye A, Buscombe J, Chatal JF, et al., *Bone scintigraphy: procedure guidelines for tumour imaging.* Eur J Nucl Med Mol Imaging, 2003. **30**(12): p. BP99-106.
2. Nathan M, Gnanasegaran G, Adamson K, and Fogelman I, *Bone Scintigraphy: Patterns, Variants, Limitations and Artefacts*, in *Radionuclide and Hybrid Bone Imaging*, I. Fogelman, G. Gnanasegaran, and H. Wall, Editors. 2012, Springer Berlin Heidelberg. p. 377-408.
3. Davies AM, Sundaram M, and James SJ, *Imaging of Bone Tumors and Tumor-Like Lesions: Techniques and Applications*. 2009: Springer-Verlag.
4. Abdel Razek AA and Castillo M, *Imaging appearance of primary bony tumors and pseudo-tumors of the spine.* J Neuroradiol, 2010. **37**(1): p. 37-50.
5. Rodallec MH, Feydy A, Larousserie F, Anract P, Campagna R, Babinet A, et al., *Diagnostic imaging of solitary tumors of the spine: what to do and say.* Radiographics, 2008. **28**(4): p. 1019-41.
6. Rodallec MH, Feydy A, Larousserie F, Anract P, Campagna R, Babinet A, et al., *Diagnostic Imaging of Solitary Tumors of the Spine: What to Do and Say.* RadioGraphics, 2008. **28**(4): p. 1019-1041.
7. International Atomic Energy Agency, *Clinical Applications of SPECT/CT: New Hybrid Nuclear Medicine Imaging System (IAEA-TECDOC-1597)*. 2008: Vienna, Austria.
8. Helyar V, Mohan HK, Barwick T, Livieratos L, Gnanasegaran G, Clarke SE, et al., *The added value of multislice SPECT/CT in patients with equivocal bony metastasis from carcinoma of the prostate.* Eur J Nucl Med Mol Imaging, 2010. **37**(4): p. 706-13.
9. Jiang L, Han L, Tan H, Hu P, Zhang Y, and Shi H, *Diagnostic value of (9)(9)mTc-MDP SPECT/spiral CT in assessing indeterminate spinal solitary lesion of patients without malignant history.* Ann Nucl Med, 2013. **27**(5): p. 460-7.
10. Patel CN, Chowdhury FU, and Scarsbrook AF, *Hybrid SPECT/CT: the end of "unclear" medicine.* Postgrad Med J, 2009. **85**(1009): p. 606-13.
11. Utsunomiya D, Shiraishi S, Imuta M, Tomiguchi S, Kawanaka K, Morishita S, et al., *Added Value of SPECT/CT Fusion in Assessing Suspected Bone Metastasis: Comparison with Scintigraphy Alone and Nonfused Scintigraphy and CT1.* Radiology, 2006. **238**(1): p. 264-271.
12. Sharma P, Sharma S, Ballal S, Bal C, Malhotra A, and Kumar R, *SPECT-CT in routine clinical practice: increase in patient radiation dose compared with SPECT alone.* Nucl Med Commun, 2012. **33**(9): p. 926-32.
13. Hara N, Onoguchi M, Takenaka K, Matsubara K, Ujita H, and Kenko Y, *Assessment of Patient Exposure to X-Radiation from SPECT/CT Scanners.* Journal of Nuclear Medicine Technology, 2010. **38**(3): p. 138-148.
14. Larkin AM, Serulle Y, Wagner S, Noz ME, and Friedman K, *Quantifying the Increase in Radiation Exposure Associated with SPECT/CT Compared to SPECT Alone for Routine Nuclear Medicine Examinations.* International Journal of Molecular Imaging, 2011. **2011**.
15. Montes C, Tamayo P, Hernandez J, Gomez-Caminero F, Garcia S, Martin C, et al., *Estimation of the total effective dose from low-dose CT scans and radiopharmaceutical administrations delivered to patients undergoing SPECT/CT explorations.* Ann Nucl Med, 2013. **27**(7): p. 610-7.

16. Griffiths M, Thompson J, Tootell A, Driver J, Kane T, Mountain V, et al., *SPECT-CT and its role in imaging and oncology.* Imaging in Oncology, Society of Radiographers, 2009.
17. Sharma P, Singh H, Kumar R, Bal C, Thulkar S, Seenu V, et al., *Bone scintigraphy in breast cancer: added value of hybrid SPECT-CT and its impact on patient management.* Nuclear Medicine Communications, 2012. **33**(2): p. 139-147.
18. International Commission on Radiological Protection, *ICRP Publication 103: Recommendations of the ICRP*. 2013: SAGE Publications.
19. International Commission on Radiological Protection, *1990 Recommendations of the International Commission on Radiological Protection: User's Edition*. 1992: International Commission on Radiological Protection.
20. GE Healthcare, *Infinifa + Hawkeye 4 User's Guide*. 2006, Buckinghamshire, UK: GE Healthcare.
21. Hiles PA, Mackenzie A, Scally A, and Wall B, *Recommended Standards for the Routine Performance Testing of Diagnostic X-ray Imaging Systems*. 2005: Institute of Physics and Engineering in Medicine.
22. Toshiba Medical Systems Corporation, *Operation Manual for Toshiba Scanner Aquillion TSX-101A Reference Volume*. 2008, Tochigi-Ken, Japan: Toshiba Medical Systems Corporation.
23. CIRS Tissue Simulation and Phantom Technology, *Adult Male Phantom Model Number 701-D Appendix 5*. 2010, CIRS, Inc: Virginia, USA.
24. CIRS Tissue Simulation and Phantom Technology. *Dosimetry Verification Phantoms Model 701-706 Data Sheet*. 2012 [cited 2012 19th January]; Available from: http://www.cirsinc.com/file/Products/701_706/701_706_DS.pdf.
25. Clark KC, Whitley AS, Sloane C, and Hoadley G, *Clark's Positioning In Radiography*. 2005: Arnold Publishers.
26. Tootell A, Szczepura K, and Hogg P. *e090: Effective Dose from Computed Tomography Attenuation Correction for Myocardial Perfusion Imaging: A comparison of Four Commonly Used systems*. United Kingdom Radiographic Congress 2013; Available from: http://ukrc2013.profile-eposters.co.uk/eposter/action/view/layout/2/id/3351.
27. ICRP, *The 2007 Recommendations of the ICRP*, in *ICRP Publication 103*. 2007, Ann. ICRP. p. 2-4.
28. Brenner DJ, *Effective dose: a flawed concept that could and should be replaced.* British Journal of Radiology, 2008. **81**(967): p. 521-523.
29. Brenner DJ, *Effective Dose- A Flawed Concept that Could and Should be Replaced*, in *International Commission on Radiological Protection*. 2011: Washington DC.
30. Wall BF, Haylock R, Jansen JTM, Hillier MC, Hart D, and Shrimpton PC, *Radiation Risks from Medical X-ray Examinations as a Function of the Age and Sex of the Patient. Report HPA-CRCE-028*. 2011, Health Protection Agency: Chilton.
31. Even-Sapir E, Flusser G, Lerman H, Lievshitz G, and Metser U, *SPECT/Multislice Low-Dose CT: A Clinically Relevant Constituent in the Imaging Algorithm of Nononcologic Patients Referred for Bone Scintigraphy.* Journal of Nuclear Medicine, 2007. **48**(2): p. 319-324.
32. Even-Sapir E, Keidar Z, and Bar-Shalom R, *Hybrid Imaging (SPECT/CT and PET/CT)—Improving the Diagnostic Accuracy of Functional/Metabolic and Anatomic Imaging.* Seminars in Nuclear Medicine, 2009. **39**(4): p. 264-275.
33. Thompson J, Hogg P, Higham S, and Manning D, *Accurate localization of incidental findings on the computed tomography attenuation correction image: the influence of tube current variation.* Nucl Med Commun, 2013. **34**(2): p. 180-4.
34. Thompson J, Hogg P, Manning D, and Szczepura K. *Lesion detection in the CT attenuation correction image of 5 different low resolution SPECT/CT systems: a multi-centre study*. in *British Nuclear Medicine Society*. 2012. Harrogate: Lippincott Williams Wilkins.
35. Thompson JD, Hogg P, Manning DJ, Szczepura K, and Chakraborty DP, *A Free-response Evaluation Determining Value in the Computed Tomography Attenuation Correction Image*

for Revealing Pulmonary Incidental Findings: A Phantom Study. Academic Radiology, 2014. **21**(4): p. 538-545.
36. Horger M, Eschmann SM, Pfannenberg C, Vonthein R, Besenfelder H, Claussen CD, et al., *Evaluation of Combined Transmission and Emission Tomography for Classification of Skeletal Lesions.* American Journal of Roentgenology, 2004. **183**(3): p. 655-661.
37. Brenner DJ, *We can do better than effective dose for estimating or comparing low-dose radiation risks.* Annals of the ICRP, 2012. **41**(3-4): p. 124-128.
38. Committee to Assess Health Risks from Exposure to Low Levels of Ionizing Radiation, Nuclear and Radiation Studies Board Division on Earth and Life Studies, and National Research Council of the National Academies, *Health Risks From Exposure to Low Levels of Ionizing Radiation: BEIR VII Phase 2*. 2006: Washington, DC.
39. Dietze G, Harrison JD, and Menzel HG, *Effective dose: a flawed concept that could and should be replaced. Comments on a paper by D J Brenner (Br J Radiol 2008;81:521–3).* British Journal of Radiology, 2009. **82**(976): p. 348-351.
40. Martin CJ, *Effective dose: how should it be applied to medical exposures?* British Journal of Radiology, 2007. **80**(956): p. 639-647.
41. Oritz P, *The use of Effective Dose in Medicine* in *The 2nd International Symposium on the System of Radiological Protection*. 2013, ICRP: United Arab Emirates.
42. Tootell A, Szczepura K, and Hogg P, *An overview of measuring and modelling dose and risk from ionising radiation for medical exposures.* Radiography, 2014. **20**(4): p. 323-332.
43. Even-Sapir E, *Imaging of Malignant Bone Involvement by Morphologic, Scintigraphic, and Hybrid Modalities*.* Journal of Nuclear Medicine, 2005. **46**(8): p. 1356-1367.
44. Ndlovu X, George R, Ellmann A, and Warwick J, *Should SPECT-CT replace SPECT for the evaluation of equivocal bone scan lesions in patients with underlying malignancies?* Nuclear Medicine Communications, 2010. **31**(7): p. 659-665.
45. Palmedo H, Marx C, Ebert A, Kreft B, Ko Y, Türler A, et al., *Whole-body SPECT/CT for bone scintigraphy: diagnostic value and effect on patient management in oncological patients.* European Journal of Nuclear Medicine and Molecular Imaging, 2014. **41**(1): p. 59-67.
46. British Nuclear Medicine Society. *Clinical Guideline for Bone Scintigraphy*. 2014 [cited 2015 4th March]; Available from: http://www.bnms.org.uk/images/stories/Procedures_and_Guidelines/BNMS_Bone_Scintigraphy_Guideline_v1.pdf.
47. Zhang Y, Shi H, Cheng D, jiang L, Xiu Y, Li B, et al., *Added value of SPECT/spiral CT versus SPECT in diagnosing solitary spinal lesions in patients with extraskeletal malignancies.* Nuclear Medicine Communications, 2013. **34**(5): p. 451-458.
48. Palmedo H, Marx C, Ebert A, Kreft B, Ko Y, Turler A, et al., *Whole-body SPECT/CT for bone scintigraphy: diagnostic value and effect on patient management in oncological patients.* Eur J Nucl Med Mol Imaging, 2014. **41**(1): p. 59-67.